

Reaction Engineering Aspects of Suspension Polymerization

ANTONIOS G. MIKOS, CHRISTOS G. TAKOUDIS, and NIKOLAOS A. PEPPAS,* *School of Chemical Engineering, Purdue University, West Lafayette, Indiana 47907*

Synopsis

Suspension polymerization is used for the production of polymer particles with diameter in the range of 50–750 μm . The particle size distribution of the particles produced in batch-suspension polymerization is calculated using a population balance model. Power laws are derived for the average particle size and the standard deviation of the distribution. It is found that both quantities scale to the stable droplet mass of the initial dispersion of the organic phase into the aqueous one, which is a function of the agitation rate and the surface tension.

INTRODUCTION

Suspension polymerization utilizes an aqueous phase where the immiscible monomer or monomers are dispersed by agitation.¹ If the agitation is stopped, the phases are often separated and the less dense phase rises to the top of the reactor (creaming). The process is also referred to as bead, pearl, or granular polymerization because of the form of the final product.

The polymerization takes place entirely in the monomer phase.² No mass transfer occurs between the monomer and the aqueous phase. The initiators used are soluble in the monomer phase and are the same as those used in bulk and solution polymerization (i.e., organic peroxides and azo-compounds). The volume ratio of the continuous aqueous phase to the dispersed organic phase^{3,4} varies from 1:1 to 6:1. Higher ratios are required in rapid polymerizations, where heat is removed in a short time.

The monomer droplets are prevented from coalescing by the use of suspending agents in the suspending phase. The suspending agents are either water-soluble organic polymers or inorganic compounds in the form of water-insoluble powders or precipitates.^{3,4} Good suspending agents are starch, proteinaceous materials, and poly(vinyl alcohol), which are very weak surfactants. Droplet coalescence may occur when two droplets collide, because of the drainage of the thin liquid film between them. When an organic compound is used as a suspending agent, a thin, gel-like, protective layer is formed, that keeps monomer droplets separated and hinders coalescence. The coalescence frequency is highly temperature dependent and increases with temperature.

The polymer particles produced in suspension polymerization have applications in chromatographic separations, ion-exchange chromatography,

* To whom all correspondence should be addressed.

biochemical and biomedical engineering, etc. In chromatographic separations such as high-pressure liquid chromatography, gel permeation chromatography, and so on, swollen porous microparticles of a specific polymer of (usually) a narrow size distribution are used to exclude certain molecules of a solution by size separation.⁵ In this case the particle size, degree of swelling, pore size, and interparticle space are very important.⁶ In ion-exchange applications the resins are usually charged with SO_3^- , NH_4^+ or related functional groups to produce anionic or cationic ion-exchange resins. The charge per area, degree of swelling, and pore size distribution are important parameters in various applications.⁷

The solubility of the polymer in its monomer determines the mechanism of particle formation and growth and its porosity. Of the many types of polymer microparticles, polystyrene microparticles are probably the most widely studied owing to their use as chromatographic (e.g., μ -Styragel[®]) or as ion-exchange resins (e.g., Amberlite[®]). They are prepared either by the classical technique of suspension copolymerization-crosslinking of styrene and divinylbenzene (DVB) or by novel techniques such as Friedel-Crafts suspension crosslinking of polystyrene using difunctional crosslinking agents.⁸⁻¹¹

Here we present a new reaction engineering model which can be used to predict the particle size of the microspheres prepared in suspension polymerization from monomers that are either good solvents for their polymers or good swelling agents for their crosslinked polymers (e.g., styrene).

MATHEMATICAL MODELING

A model is presented to account for the dispersion of monomer droplets and their gradual transformation into polymer particles in a batch-suspension polymerization reaction. The kinetic model for copolymerization-crosslinking reactions was developed by Mikos¹² and it was used to calculate the number average molecular weight between crosslinks, \bar{M}_c , the number average molecular weight, \bar{M}_n , and the average number of effective crosslinks per chain, ν_e , as a function of time.

The reaction engineering model developed here accounts for the size distribution of the particles of polymer during the reaction as a function of agitation rate, surface tension and initial droplet distribution. In contrast with emulsion polymerization,¹³ the agitation rate in suspension polymerization determines the particle size distribution, as it causes the dispersion of the organic phase in the aqueous one. This dispersion is not stable due to the existence of droplet breakage and coalescence. Droplet coalescence is hindered by using suspending agents. The droplet breakage reduces the size of the droplets down to a stable size.

Shinnar¹⁴ calculated the stable droplet mass, m_s , based on Kolmogoroff's theory of local isotropy, when the droplets are larger than the microscale of turbulence (a few μm), so that the shear forces can be neglected.

$$m_s = K \pi \rho^{-4/5} \sigma_i^{9/5} (N_i^2 D_i^{4/3})^{-9/5} \quad (1)$$

Here, K is a constant depending on the vessel geometry, ρ is the dispersed phase density, σ_i is the interfacial tension, N_I and D_I are the impeller speed and diameter, respectively. Equation (1) is applicable when the densities and the viscosities of both phases are approximately equal. The reader should recall that the size of the particles produced in suspension polymerization is hundreds of microns in diameter.

A population balance model is used to calculate the droplet mass distribution of the liquid dispersion. It is assumed that there is no droplet coalescence. The population balance equation is:

$$\frac{\partial n(\xi, t)}{\partial t} = \int_{\xi}^{\infty} \nu(\mu) \gamma(\mu) \beta(\xi, \mu) n(\mu, t) d\mu - \gamma(\xi) n(\xi, t) \quad (2)$$

Here, $n(\xi, t) d\xi$ is the number of droplets with normalized mass between ξ and $\xi + d\xi$ at time t . The reference mass is the stable droplet mass, which is given in Eq. (1).

$$\xi = \frac{m}{m_s} \quad (3)$$

Furthermore, $\nu(\xi)$ is the average number of daughter droplets upon breakage of a droplet of mass ξ ; $\gamma(\xi) dt$ is the breakage probability, that is, the probability that a droplet of normalized mass ξ will break in the time interval t and $t + dt$; and $\beta(\xi, \mu)$ is the daughter droplet probability, that is, the probability that a droplet of mass ξ will be formed by breakage of a droplet of mass μ .

The first term of the right hand side of Eq. (2) corresponds to the production of droplets of normalized mass ξ , due to the breakage of larger droplets. The second term corresponds to the consumption of droplets of the mass ξ , due to their breakage.

Population balances¹⁵ have been used extensively to study liquid-liquid dispersions. Amundson and his collaborators^{16,17} developed a population balance model to relate the droplet breakage and coalescence in dispersed phase systems. Referring to the central limit theorem of the probability theory it was assumed that the daughter droplet probability was a normal function,

$$\beta(\xi, \mu) = \frac{1}{\sigma(2\pi)^{1/2}} \exp\left[-\frac{(\xi - \bar{\xi})^2}{2\sigma^2}\right] \quad (4)$$

where $\bar{\xi}$ is the average mass of the daughter droplets upon breakage of a droplet of mass μ .

$$\bar{\xi} = \frac{\mu}{\nu(\mu)} \quad (5)$$

The standard deviation, σ , is chosen such that the daughter droplet distribution lies essentially within the range from 0 to μ . It can be assumed that

$$\sigma = c\bar{\xi} \quad (6)$$

where c is a proportionality constant, which can be regarded as a parameter

depending on the operating conditions. The integral $\int_0^{\mu} \beta(\xi, \mu) d\xi$ is equal¹⁸

to 0.9876 or approximately equal to 1 using $c = 0.4$ for binary breakage ($\nu(\mu) = 2$). Therefore, the value of c equal to 0.4 can be regarded as a threshold value, such that normalization of the distribution will be required for higher values. As the parameter c decreases, the distribution becomes narrower and the probability function is reduced to a delta function for the limiting value of c equal to zero, which implies a discrete breakage process. In this work the parameter c is set equal to 0.4.

Narsimhan et al.¹⁹ proposed a model for the breakage probability based on the droplet breakage due to its oscillation resulting from the relative velocity fluctuations.

$$\gamma(\xi) = \begin{cases} 0 & \xi \leq 1 \\ \lambda \operatorname{erfc}(3.5\xi^{-5/18}) & \xi > 1 \end{cases} \quad (7)$$

where λ is the frequency of eddies arriving on the droplet surface, which is assumed to be constant. Equation (7) is applicable when the droplet is larger than the microscale of turbulence.

The total number of droplets at time t , $N(t)$, is:

$$N(t) = \int_0^{\infty} n(\mu, t) d\mu \quad (8)$$

The conservation equation for the total number of droplets is

$$\frac{dN(t)}{dt} = \int_1^{\infty} [\nu(\mu) - 1] \gamma(\mu) n(\mu, t) d\mu \quad (9)$$

The fraction of droplets with mass between ξ and $\xi + d\xi$ at time t , $f(\xi, t)d\xi$, is

$$f(\xi, t)d\xi = \frac{n(\xi, t)d\xi}{N(t)} \quad (10)$$

The left hand side of Eq. (2) can be written as

$$\frac{\partial n(\xi, t)}{\partial t} = N(t) \frac{\partial f(\xi, t)}{\partial t} + f(\xi, t) \frac{dN(t)}{dt} \tag{11}$$

Then, Eq. (2) becomes:

$$\begin{aligned} \frac{\partial f(\xi, t)}{\partial t} = & \int_{\xi}^{\infty} v(\mu) \gamma(\mu) \beta(\xi, \mu) f(\mu, t) d\mu \\ & - f(\xi, t) [\gamma(\xi) + \int_1^{\infty} [v(\mu) - 1] \gamma(\mu) f(\mu, t) d\mu] \end{aligned} \tag{12}$$

A simulation time, τ , is defined as follows:

$$\tau = 10^{-3} \lambda t \tag{13}$$

where 10^{-3} is a scaling factor. Then, Eq. (12) becomes:

$$\begin{aligned} \frac{\partial \bar{f}(\xi, \tau)}{\partial \tau} = & \int_{\xi}^{\infty} v(\mu) \bar{\gamma}(\mu) \beta(\xi, \mu) \bar{f}(\mu, \tau) d\mu \\ & - \bar{f}(\xi, \tau) [\bar{\gamma}(\xi) + \int_1^{\infty} [v(\mu) - 1] \bar{\gamma}(\mu) \bar{f}(\mu, \tau) d\mu] \end{aligned} \tag{14}$$

where the normalized breakage probability, $\bar{\gamma}(\xi)$, is:

$$\bar{\gamma}(\xi) = \begin{cases} 0 & \xi \leq 1 \\ 10^3 \operatorname{erfc}(3.5 \xi^{-5/18}) \xi & \xi > 1 \end{cases} \tag{15}$$

The calculation of the particle size distribution is uncoupled from the polymerization reaction itself, if the polymerization is initiated once a stable dispersion is formed. Then, each droplet behaves as a segregated batch reactor. The droplet mass distribution is controlled by the stable droplet mass before the polymerization initiation, m_s , which is a lumped parameter of the surface tension, σ_i , the impeller speed, N_I , and the impeller diameter, D_I . The surface tension, σ_i , refers to the monomer-water interface and it is not constant during the polymerization. Once the polymerization reaction has started the viscosity of the dispersed phase is increased, therefore, Eq. (1) is not valid. The particle size distribution, $g(v, t)$, is:

$$g(v, t) = \frac{\rho}{m_s} \bar{f}(\rho v / m_s, 10^{-3} \lambda t) \tag{16}$$

where $g(v,t)dv$ is the fraction of particles with volume between v and $v + dv$ at time t . Also, ρ is the polymer particle density, which changes during the polymerization.

Finally, the initial distribution of the droplets depends on the medium used for the dispersion of the organic phase in the aqueous phase. If an atomizer is used, we can approximate the initial differential mass distribution with a logarithmic normal one.²⁰

$$\bar{f}(\xi,0) = \frac{1}{\xi\sigma(2\pi)^{1/2}} \exp\left[-\frac{(\ln\xi - \ln\xi_m)^2}{2\sigma^2}\right] \quad (17)$$

Here, ξ_m is the median of the distribution and σ is the standard deviation²¹ of $\ln\xi$.

RESULTS AND DISCUSSION

In order to predict the particle size distribution of the polymer particles formed in batch-suspension polymerization we postulate that the polymerization reaction is initiated once a stable dispersion is formed. Thus, the calculation of the droplet mass distribution does not depend on the polymerization reaction and the control of the particle size distribution is easier.

The particle size distribution can be evaluated from the droplet mass distribution, as shown in Eq. (16), assuming that the unreacted monomer swells the produced polymer. The density of the polymer particles changes during the polymerization reaction according to Eq. (18).

$$\frac{d\rho}{dt} = -\left[r_M w \left(\frac{1}{\rho_m} - \frac{1}{\rho_p}\right)\right] \rho \quad (18)$$

Here, r_M is the monomer reaction rate, w is the monomer molecular weight, ρ is the density, and the subscripts m and p correspond to monomer and polymer, respectively. Similar relations have been developed by Mikos¹² for the copolymerization reaction.

If the polymerization is initiated before a stable dispersion is formed, it is possible that large monomer droplets will be stabilized due to the developing viscous forces. The heat transfer from such big droplets might be insufficient, thus causing runaway problems.

The differential droplet mass distribution was calculated by solving numerically the population balance equation. To solve the integral-differential Eq. (14), a numerical integration and collocation method²² was used. One hundred collocation points were used to span the interval from 0 to 10 in ξ . The points were equally spaced. Both integrals were approximated using Simpson's rule²³ and the resulting system of 100 ordinary differential equations was solved along the collocation points using the Adams method. The convergence of the solution was checked by using different numbers of collocation points (e.g., 80 points).

The breakage process was assumed to be binary. Thus, the average number of daughter droplets, $\nu(\mu)$, upon breakage of a droplet of mass μ is equal to two.

$$\nu(\mu) = 2 \quad (19)$$

The time evolution of the differential droplet mass distribution for different initial distributions is shown in Figures 1 through 3. It is assumed that the initial distribution is not limited to the interval from 0 to 1 in ξ . In general, the distribution depends on the shape of the initial distribution at small times, as shown for the values of the simulation time, τ , equal to 0.5 and 1. However, at large times because of the randomness of the breakage process it becomes independent of the shape of the initial distribution and it is symmetric and quasnormal. In lean dispersions, where droplet coalescence is minimal, the equilibrium distribution was a normal function.²⁴

In all transient distributions there exists an uptake in the region from 0 to 1. This is explained by the accumulation of the droplets with dimen-

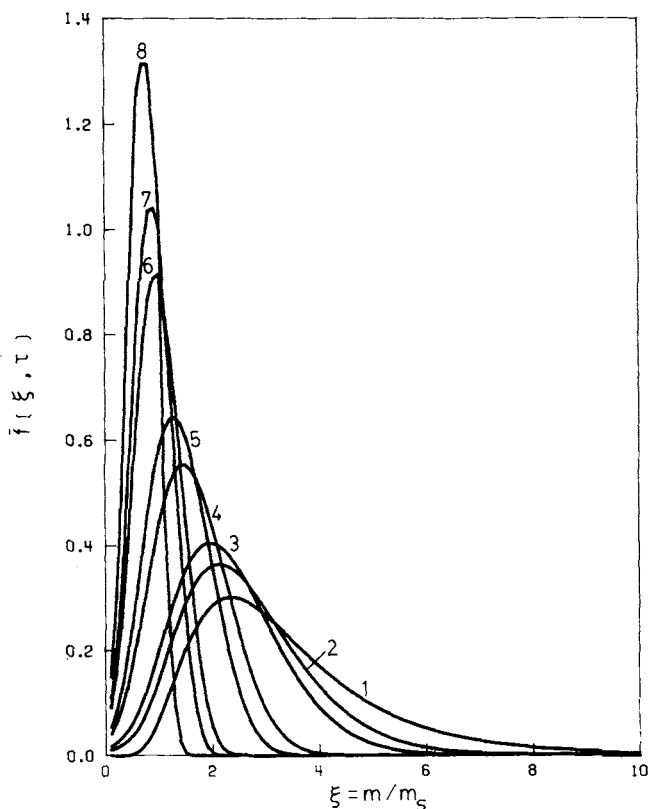


Fig. 1. Effect of the simulation time, τ , on the differential droplet mass distribution, $\bar{f}(\xi, \tau)$ (the initial distribution is logarithmic normal with $\xi_m = 3$ and $\sigma = 0.5$). Eight different times were used: $\tau = 0.0$ (curve 1), $\tau = 0.5$ (curve 2), $\tau = 1.0$ (curve 3), $\tau = 5.0$ (curve 4), $\tau = 10.0$ (curve 5), $\tau = 50.0$ (curve 6), $\tau = 100.0$ (curve 7), $\tau = 500.0$ (curve 8).

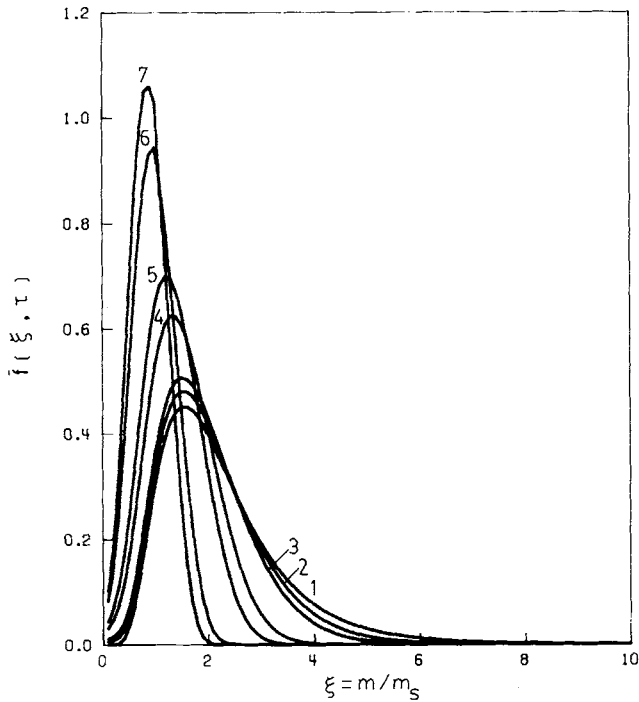


Fig. 2. Effect of the simulation time, τ , on the differential droplet mass distribution, $\bar{f}(\xi, \tau)$ (the initial distribution is logarithmic normal with $\xi_m = 2$ and $\sigma = 0.5$). Seven different times were used: $\tau = 0.0$ (curve 1), $\tau = 0.5$ (curve 2), $\tau = 1.0$ (curve 3), $\tau = 5.0$ (curve 4), $\tau = 10.0$ (curve 5), $\tau = 50.0$ (curve 6), $\tau = 100.0$ (curve 7).

sionless mass, ξ , in the range of 0 to 1. These droplets, resulting from the breakage of larger droplets, are stable and do not break further. In other

words, the integral $\int_{\xi_1}^{\xi_2} \bar{f}(\xi, \tau) d\xi$ for $0 \leq \xi_1 < \xi_2 \leq 1$ increases as the simulation time increases.

The effects of the parameters ξ_m and σ of the initial distribution on the mean, $\bar{\xi}$, and the standard deviation, $\sigma^{\bar{f}}$, of the transient differential distributions, $\bar{f}(\xi, \tau)$, are shown in Figures 4 and 5, respectively. It is seen that for simulation times, τ , larger than 10 the values of $\bar{\xi}$ and $\sigma^{\bar{f}}$ become independent of the initial conditions, and the values of $\bar{\xi}$ are approximately equal to each other, as are the values of $\sigma^{\bar{f}}$. However, the differential droplet mass distribution is evaluated in terms of the dimensionless mass ξ . The particle size distribution, $g(v, t)$, depends on the value of the stable droplet mass, as shown in Eq. (16). The average particle size, \bar{v} , and the standard deviation, σ^g , of the particle size distribution, $g(v, t)$, are:

$$\bar{v} = \frac{m_s}{\rho} \bar{\xi} \quad (20)$$

$$\sigma^g = \frac{m_s}{\rho} \sigma^{\bar{f}} \quad (21)$$

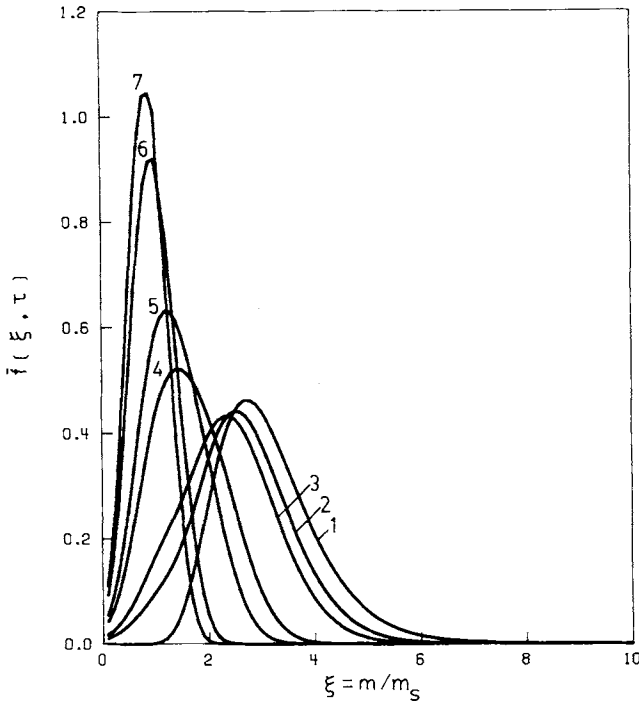


Fig. 3. Effect of the simulation time, τ , on the differential droplet mass distribution, $\bar{f}(\xi, \tau)$ (the initial distribution is logarithmic normal with $\xi_m = 3$ and $\sigma = 0.3$). Seven different times were used: $\tau = 0.0$ (curve 1), $\tau = 0.5$ (curve 2), $\tau = 1.0$ (curve 3), $\tau = 5.0$ (curve 4), $\tau = 10.0$ (curve 5), $\tau = 50.0$ (curve 6), $\tau = 100.0$ (curve 7).

Consequently, the smaller the stable droplet mass, the smaller the average particle size, and the narrower the particle size distribution.

Thus, according to Eq. (1), high impeller speeds and small surface tensions give rise to small average particle sizes, a conclusion which is confirmed by experimental data.²⁵ Therefore, the use of a surfactant which reduces the monomer-water surface tension results essentially in the production of small sizes of polymer particles of a narrow distribution.

The particle density, ρ , is constant at the end of the polymerization reaction (approximately equal to that of the polymer). Therefore, assuming that the polymerization reaction is initiated once a stable dispersion is formed, namely when the values of $\bar{\xi}$ and σ^2 become independent of the initial droplet mass distribution, Eqs. (20) and (21) give the power laws

$$\bar{v} \sim \bar{d}^3 \sim m_s \quad (22)$$

where \bar{d}^3 is the average value of the cube of the particle diameter, d , and

$$\sigma^2 \sim m_s \quad (23)$$

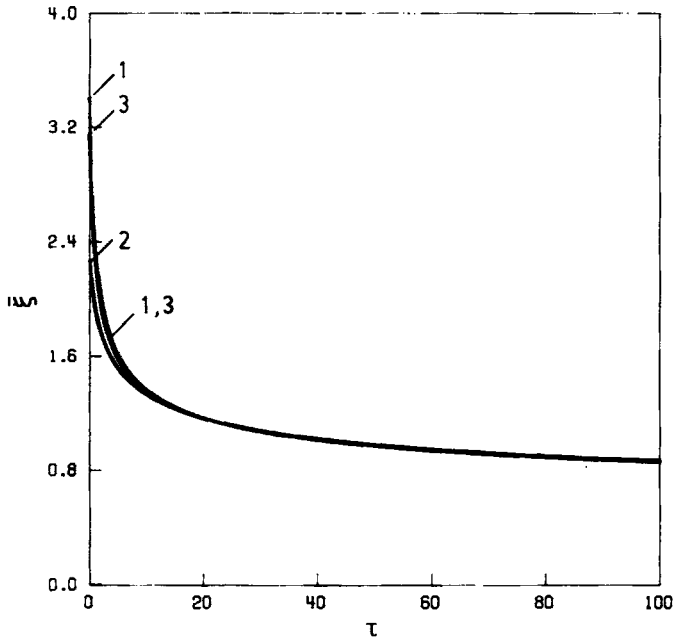


Fig. 4. Effect of the parameters ξ_m and σ of the initial distribution on the mean, $\bar{\xi}$, of the transient differential distributions, $\bar{f}(\xi, \tau)$. Three different initial conditions were used: $\xi_m = 3$, $\sigma = 0.5$ (curve 1); $\xi_m = 2$, $\sigma = 0.5$ (curve 2); $\xi_m = 3$, $\sigma = 0.3$ (curve 3).

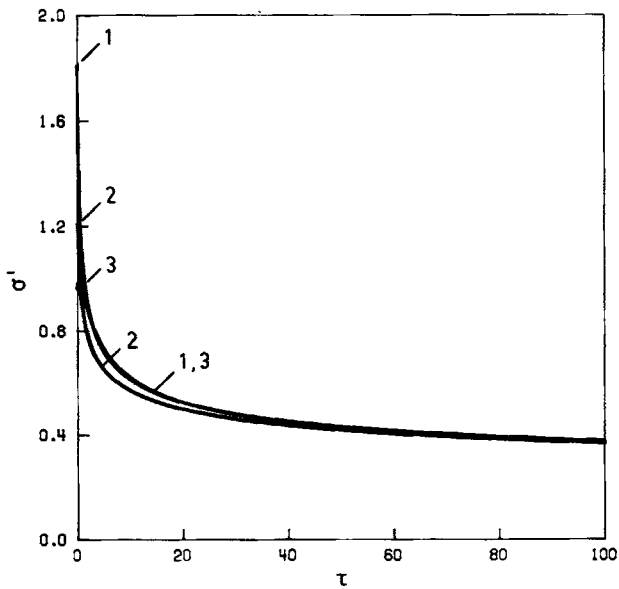


Fig. 5. Effect of the parameters ξ_m and σ of the initial distribution on the standard deviation, σ^f of the transient differential distributions, $\bar{f}(\xi, \tau)$. Three different initial conditions were used: $\xi_m = 3$, $\sigma = 0.5$ (curve 1); $\xi_m = 2$, $\sigma = 0.5$ (curve 2); $\xi_m = 3$, $\sigma = 0.3$ (curve 3).

Using Eq. (1) we obtain

$$\bar{v} \sim \bar{d}^3 \sim \sigma_i^{9/5} (N_i^2 D_i^{4/3})^{-9/5} \quad (24)$$

$$\sigma^g \sim \sigma_i^{9/5} (N_i^2 D_i^{4/3})^{-9/5} \quad (25)$$

The surface tension in the power laws is that before the polymerization is initiated and not that during the polymerization. Furthermore, one may write

$$\sigma^g \sim \bar{v} \quad (26)$$

Thus, it is concluded that the average particle size and the standard deviation of the particle size distribution cannot be controlled simultaneously either by the agitation rate or by the surface tension. Therefore, with the assumptions of the proposed model, large particles in a narrow range cannot be produced in batch suspension polymerization.

Finally, the preceding analysis is valid when the stable droplet mass during the polymerization is larger than that before the polymerization is initiated. The reader should recall that Eq. (1) is not valid during the polymerization because it assumes that the viscosities of both phases are approximately equal.

CONCLUSIONS

A reaction engineering model was developed for the batch-suspension polymerization of monomers that are either good solvents for their polymers or good swelling agents for their crosslinked polymers, so as not to have phase separation during the polymerization. For example it can be used to calculate the particle size distribution of crosslinked polystyrene beads produced in suspension polymerization. However, it is not applicable to polymerizations where a separation of phases occurs like that of vinyl chloride.

The effects of the characteristics of agitation, such as the impeller speed and the impeller diameter, as well as the surface tension of the reacting medium on the particle size distribution were investigated. It was found that the average size and the standard deviation of the particle size distribution scale to the same quantity, which is a lumped parameter of the monomer density, the impeller speed, the impeller diameter, and the surface tension of the dispersion before the polymerization reaction is initiated.

We wish to acknowledge significant contributions of Todd E. Wilke in the development of the numerical solutions of this paper.

NOTATION

c	Proportionality constant.
d	Particle diameter.
\bar{d}^3	Third moment about origin of a distribution of the particle diameter, d .

D_I	Impeller diameter.
$f(\xi, t), \bar{f}(\xi, \tau)$	Differential mass distribution of droplets.
$g(v, t)$	Particle size distribution.
K	Constant depending on the vessel geometry.
m	Droplet mass.
m_s	Stable droplet mass.
$n(\xi, t)$	Droplet mass distribution.
$N(t)$	Total number of droplets.
N_I	Impeller speed.
r_M	Reaction rate.
t	Time.
v	Particle volume.
\bar{v}	Average value of a distribution of v .
w	Molecular weight.

Greek Letters

$\beta(\xi, \mu)$	Daughter droplet probability.
$\gamma(\xi)$	Breakage probability.
$\bar{\gamma}(\xi)$	Normalized breakage probability.
λ	Frequency of eddies arriving on a droplet surface.
$\nu(\mu)$	Average number of daughter droplets upon breakage of a droplet of mass μ .
$\underline{\xi}$	Dimensionless mass.
$\bar{\xi}$	Average value of a distribution of ξ .
ξ_m	Median value of a distribution of ξ .
ρ	Density.
σ	Standard deviation of a distribution.
σ_i	Interfacial tension.
τ	Simulation time.

Subscripts

p	Polymer.
m	Monomer.

Superscripts

\bar{f}	$\bar{f}(\xi, \tau)$.
\bar{g}	$\bar{g}(v, t)$.

References

1. W. H. Ray and R. L. Laurence, in *Chemical Reactor Theory; A Review*, L. Lapidus and N. R. Amundson, Eds., Prentice Hall, Englewood Cliffs, N.J., 1977.
2. G. Odian, *Principles of Polymerization*, McGraw Hill, New York, 1970.
3. E. Trommsdorff and C. E. Schildknecht, in *Polymer Processes*, C. E. Schildknecht, Ed., High Polymers, Vol. 10, 69, Interscience, New York, 1956.
4. M. Munzer and E. Trommsdorff, in *Polymerization Processes*, C. E. Schildknecht and I. Skeist, Eds., High Polymers, Vol. 29, 106, Wiley, New York, 1977.
5. K. H. Altgelt, in *Advances in Chromatography*, Vol. 7, 3, Dekker, New York, 1968.
6. C. Hirayama, M. Iida, and Y. Motozato, *Polymer*, **22**, 1561 (1981).
7. S. Patell and J. C. R. Turner, *J. Separ. Proc. Technol.*, **1**(2), 31 (1980).

8. W. R. Bussing and N. A. Peppas, *Polymer*, **24**, 209 (1983).
9. W. R. Bussing and N. A. Peppas, *Polymer*, **24**, 898 (1983).
10. D. G. Barar, K. P. Staller, and N. A. Peppas, *Ind. Eng. Chem., Prod. Res. Dev.*, **22**, 161 (1983).
11. D. G. Barar, K. P. Staller, and N. A. Peppas, *J. Polym. Sci., Polym. Chem.*, **21**, 1013 (1983).
12. A. G. Mikos, M.S.Ch.E. thesis, School of Chemical Engineering, Purdue University, 1985.
13. K. W. Min and W. H. Ray, *J. Macromol. Sci.-Revs. Macromol. Chem.*, **C11**, 177 (1974).
14. R. Shinnar, *J. Fluid Mech.*, **10**, 259 (1961).
15. H. M. Hulburt and S. Katz, *Chem. Eng. Sci.*, **19**, 555 (1964).
16. K. J. Valentas, O. Bilous, and N. R. Amundson, *Ind. Eng. Chem. Fund.*, **5**, 271 (1966).
17. K. J. Valentas and N. R. Amundson, *Ind. Eng. Chem. Fund.*, **5**, 533 (1966).
18. M. R. Spiegel, *Mathematical Handbook*, Schaum's Outline Series, McGraw Hill, New York, 1968, p. 257.
19. G. Narsimhan, J. P. Gupta, and D. Ramkrishna, *Chem. Eng. Sci.*, **34**, 257 (1979).
20. R. A. Mugele and H. D. Evans, *Ind. Eng. Chem.*, **43**, 1317 (1951).
21. L. H. Peebles, Jr., in *Polymer Reviews*, H. F. Mark and E. H. Immergut, Eds., Vol. 18, Interscience, New York, 1971.
22. G. Dahlquist and A. Bjorck, *Numerical Methods*, N. Anderson, Trans., Prentice Hall, Englewood Cliffs, NJ, 1974.
23. B. Carnahan, H. A. Luther, and J. O. Wilkes, *Applied Numerical Methods*, Wiley, New York, 1969.
24. H. T. Chen and S. Middleman, *A.I.Ch.E. J.*, **13**, 989 (1967).
25. T. Balakrishnan and W. T. Ford, *J. Appl. Polym. Sci.*, **27**, 133 (1982).

Received October 15, 1985

Accepted January 3, 1986